POLYLACTIC ACID (PLA) – NANO ALUMINA COMPOSITE POLYMER FOAMS VIA COMBINED SOLID STATE FOAMING AND ADDITIVE MANUFACTURING

Mohammed Syed Mustafa, Mitchell Owen, Sriharsha Sundarram
Fairfield University
Fairfield, CT

ABSTRACT

Polylactic acid (PLA) is one of the most widely used thermoplastic. The goal of this study is to fabricate PLA-alumina nanocomposite foams via solid state foaming of additively manufactured structures for applications that require light weight material with higher strength. PLA – nano alumina suspensions with varying compositions were prepared by ultrasonic stirring followed by solvent extraction to obtain thin films. The thin films were subsequently fed into an extruder to obtain filament for 3D printing. The filament was used to print specimens with desired architectures which were subjected to solid state foaming to generate the porous structure. The foamed and un-foamed specimens were subjected to a tensile test using the ASTM D638 and ASTM D882 standard to study the effect of solvent (DCM, DMF), alumina percentage (0, 5, 10) and porosity on strength of the samples. Scanning electron microscopy was used to measure the average pore size of the foamed samples. The results showed that the addition of alumina improves the strength of foamed samples, however the percentage increase depends on the solvent. The maximum tensile strength of foamed 10 wt% alumina nano composites prepared using DCM was measured to be around 75% higher than pure PLA foams.

Keywords: Solid state foaming, Additive manufacturing, Poly lactic acid
Corresponding author: Sriharsha Sundarram

1. INTRODUCTION

Polymers are used in a variety of applications spanning consumer products, automotive, healthcare to aerospace. The main advantage that polymers offer is a strength to weight ratio comparable to metals satisfying functional requirements of many applications. However, their properties can be significantly enhanced with the addition of nanoparticles which have a similar length scale as polymers resulting in synergistic polymer nanocomposites with superior mechanical, thermal, and electrical properties. Further, these polymer nanocomposites could be converted into nanocomposite foams which offer the enhanced properties of nanocomposites along with inherent light weight nature of foams for aerospace and structural applications.

1.1 Polymer Nanocomposite Foams

Different types of nanoparticles such as carbon nano tubes [1,2], carbon nano fibers [3,4], nano alumina [5,6], nano clay [7,8], nano silica [9,10], and graphene [11,12] have been reported to be used to enhance the properties of polymers. These nanocomposites have been fabricated using

approaches such as solution blending [13], melt blending [14], and in-situ polymerization [15]. These techniques typically result in either thin films or sheets as the end product.

Polymer foams are two phase materials with the solid polymer matrix and the gaseous pores forming the two phases respectively [16]. Polymer foams are commonly processed using techniques such as melt processing with blowing agents [17,18], emulsification/freeze drying [19], solvent casting [20], and thermal-induced phase separation [21]. These techniques could possibly be used to obtain polymer nanocomposite foams but do not provide good control over the pore size and result in mostly thin films only. The alternate technique that is gaining wide spread attention to fabricate thermoplastic polymer nanocomposite foams is solid state foaming [17]. Solid state foaming allows to generate porous structure in any thermoplastic sample irrespective of the shape or size. The two major steps in this process are: (a) saturation of the polymer matrix with a high pressure gas (typically CO_2 or N_2) and (b) nucleating bubbles in the system by creating a thermodynamic instability. The bubbles are typically nucleated using either a sudden increase in temperature or a sudden drop in pressure. Studies have shown that the presence of nano additives aids in bubble nucleation as they create more nucleation sites in the polymer matrix [22]. Solid state foaming has been used to foam thermoplastic polymers such as polylactic acid (PLA) [23], poly-(methyl methacrylate) (PMMA) [24], polyetherimide (PEI) [25], styrene acrylonitrile (SAN) and polyurethane (PU) [26].

1.2 Fused Deposition Modeling

Fused deposition modeling (FDM), commonly known as 3D printing is an additive manufacturing technique that can be used to fabricate components from polymer and polymer nanocomposite filaments [27]. The major advantage that this technique offers is the ability to fabricate components with any shape and orientation in a straightforward and cost effective manner from a computer-aided design (CAD) file. The most commonly used materials for 3D printing are polylactic acid (PLA) [28] and acrylonitrile butadiene styrene (ABS) [29].

1.3 Goals and Objectives

There has been an increased demand for polymer bio composites to support growing emphasis on stringent environmental and waste management policies in place worldwide. Polylactic acid is one of the popular thermoplastic biopolymers that is used for applications such as 3D printing filament, packaging material, and medical devices. However, the ultimate strength of PLA is only around 50 MPa, which restricts its use for applications requiring higher strength values. The goal of this study is to combine 3D printing and solid state foaming to fabricate PLA-alumina nanocomposite foams with improved mechanical properties and reduced weight. There is evidence from literature stating that alumina enhances the mechanical properties of polylactic acid. Drawbacks of those techniques include not being cost effective and lack of testing on mechanical properties. In this study, PLA-alumina suspensions were prepared by ultrasonic stirring and solvent extraction approach used to obtain thin films, which were subsequently fed into an extruder to obtain 3D printing filament. The filament is used to print dumbbell specimens for mechanical property testing as per ASTM D638 standard. The 3D printed specimens were subjected to gas saturation and subsequently foamed with glycerin to generate the porous structure. The average pore size was measured to be around 50 μm in these foams utilizing scanning electron microscopy.

2. EXPERIMENTATION

2.1 Materials

The polymer used in this study is polylactic acid (PLA) which is a non-polar and hydrophobic, bio-thermoplastic produced from natural resources such as corn, cassava, sugar cane or beets. PLA was chosen as the material for this study because it can be additively manufactured (3D printed) and also foamed using solid state foaming. This study used Poly(L-lactide) 4043D (referred to as PLA in this work, sourced from NatureWorks LLC, USA) with 94% L-lactic acid content. The physical properties of PLA4043D are summarized in Table 1. Alumina nano particles with commercial name NanoArc® (Alfa Aesar, USA) were used as procured. These alumina nano particles are in a powder form with a mean size of 40 – 50 nm. The two solvents used in this study are dichloromethane (DCM ACS reagent, Millipore Sigma) and dimethylformamide (DMF, Millipore Sigma).

Table 1. Physical properties of PLA4043D [30]

Property	Value
Density	1.24 g/cc
Peak melt temperature	150 °C
Glass transition temperature	55 °C
Molecular weight	67 kDa

2.2 Processing

The composite specimens are prepared as shown in the schematic in Figure 1 and explained in detail below.

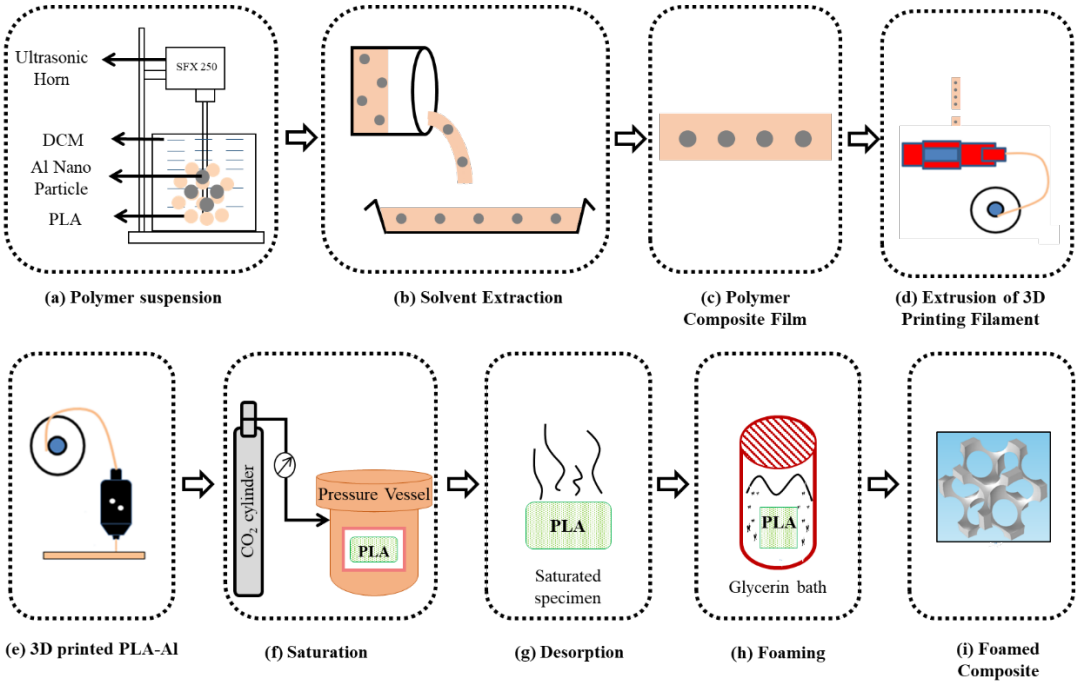

Figure 1. Schematic for fabrication of foamed polylactic acid - alumina nanocomposite foams

2.2.1 Solvent Extraction

Initially, the desired amount of solvent, either DCM or DMF was heated to 40 °C using a hot plate. The polymer to solvent ratio used in this study is 1:12 by weight. In specific, 98±2 ml of solvent was used. To the heated solvent, the alumina particles were added slowly to avoid chunking and ensure uniform dispersion by constantly stirring with a magnetic stirrer. Three different compositions of the nano particles were used: 0, 5 and 10 wt% of the polymer. Once the alumina particles were dispersed, PLA pellets were gradually added in increments of 2.5 g for a total of 10 g. All experiments in this study used 10 g PLA. The suspension was mixed thoroughly using an ultrasonic homogenizer (Branson SFX 250) at a power of 125 W for 60 minutes. After the pellets were dissolved, the solution was cast in a glass mold avoiding air bubbles. The mold was left for 48 hours to allow the solvent to fully evaporate and obtain the PLA-alumina nanocomposite film. The weight of the composite film was measured to ensure that the solvent had been extracted fully.

2.2.2 Additive Manufacturing

The composite film was cut into strips and subsequently subject to extrusion to obtain 3D printing filament. Noztek Touch HT filament extruder was used to obtain the filament. The temperatures in the die zone (T1) and barrel zone (T2) were set at 170 °C as shown in Figure 2(a). The motor speed was fixed at 15 rpm. A custom designed and 3D printed apparatus was used as a filament guide to draw the filament gradually with a uniform diameter as shown in Figure 2(b). The conical section is used to divert the air from the fan to cool the filament. This filament was used to additively manufacture (3D print) tensile test specimens. Makerbot Replicator+ printer along with their Experimental Extruder was utilized for printing the samples. The extruder head temperature and travel speed were set at 220 °C and 130 mm/s respectively to provide enough time for bonding between the deposited layers. Specimens were printed vertically with 45° on-edge orientation, 95% infill, 210 μm layer height, and diamond in-fill pattern.

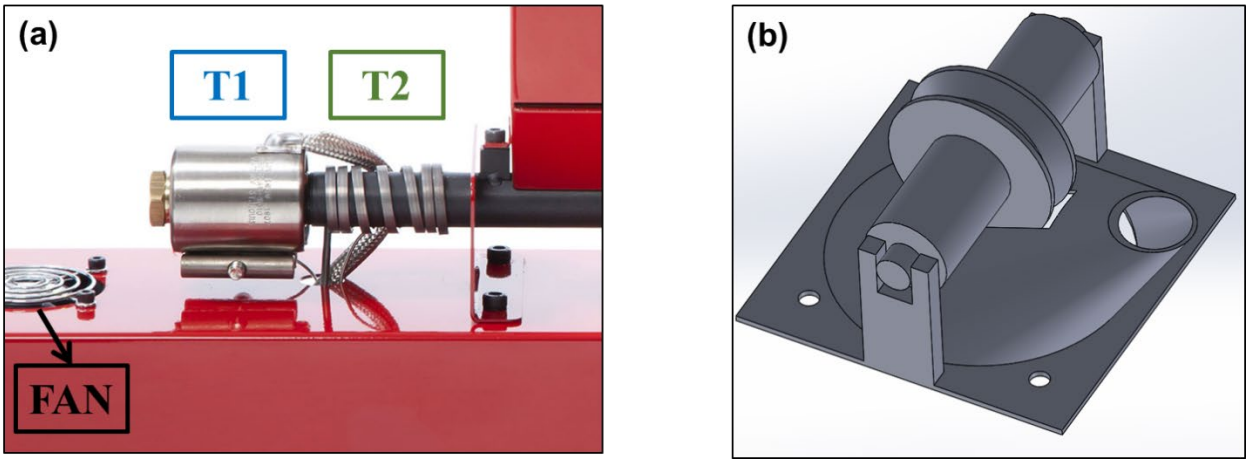

Figure 2. Extruder showing (a) die and barrel zone and (b) solid model of filament guide

2.2.3 Solid State Foaming

The 3D printed specimens and the films obtained after solvent extraction were then subjected to solid state foaming to obtain porous nanocomposites. The solid state foaming parameters for PLA were determined by our group in a prior study [23]. The samples were wrapped with a thin layer

of polyvinyl chloride (PVC) film to minimize gas desorption [31] and saturated with 2.5 MPa carbon dioxide (CO_2) for 2 hours. The weight of the samples were measured before and after saturation to determine the gas saturation percentage. The gas saturated samples were foamed in glycerin for 10 seconds at 90 °C.

A summary of all the experiments is given in Appendix – A.

2.3 Characterization

2.3.1 Tensile Testing

The films as obtained after solvent extraction were cut into 17.2 mm * 50.4 mm rectangles to test as per ASTM D882 (Standard Test Method for Tensile Properties of Thin Plastic Sheeting) [32] standard. The 3D printed dumbbell specimens were tested as per ASTM D638 (Standard Test Method for Tensile Properties of Plastics) [33] standard. The two tests were used to determine the yield strength and elongation at break using ZwickRoell Z005 universal testing machine.

2.3.2 Morphological Analysis

Foamed samples were freeze fractured with nitrogen to study the cross section using Topcon ABT 60 scanning electron microscope (SEM) equipped with energy dispersive x-ray spectroscopy (EDS). The samples were sputter coated with gold prior to observation in the SEM. The morphology, pore size, and dispersion were studied.

3. RESULTS

The main observations made during fabrication of the PLA - alumina nanocomposite foams are discussed below.

3.1 Effect of Solvent

The initial results showed that after solvent extraction, use of DCM resulted in a film with a thickness of 500 μm whereas DMF resulted in samples with powder consistency as shown in Figure 3. The cross sections of the nanocomposite films obtained from DCM were observed under the SEM to check for any alumina clusters and none were noticed. In addition, EDS area scans on different sections of the specimen showed similar alumina counts, indicating that the particles were dispersed properly.

The as obtained nano composites either in the form of film or powder were extruded into 3D printing filament. The filament was used to print dumbbell shaped specimens with 0, 5 and 10 wt% of alumina to test as per ASTM D638 for yield strength determination. The results of this test are shown in Figure 4. The results show that the effect of molecular bonding interaction is higher in the presence of DCM than DMF. Yield strength of DMF composite decreased with the addition of alumina and this shows that the DMF does not support PLA-alumina bonding effectively at molecular level. On the other hand, composites prepared using DCM showed increase in yield strength. Hence forth, all samples used for further processing were prepared with DCM as solvent which resulted in thin films.

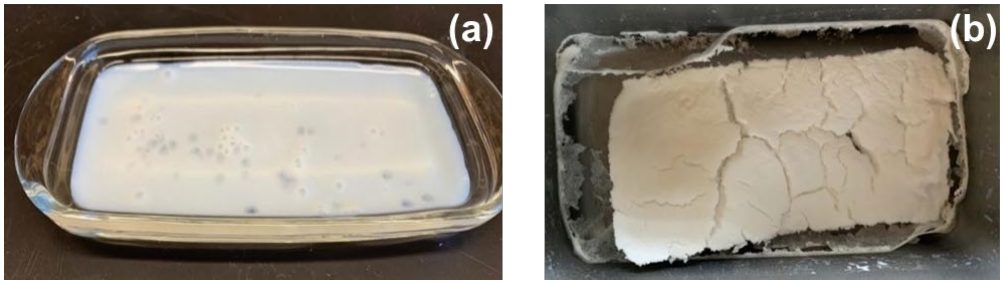

Figure 3. Samples obtained after solvent extraction using (a) dichloromethane and (b) dimethylformamide

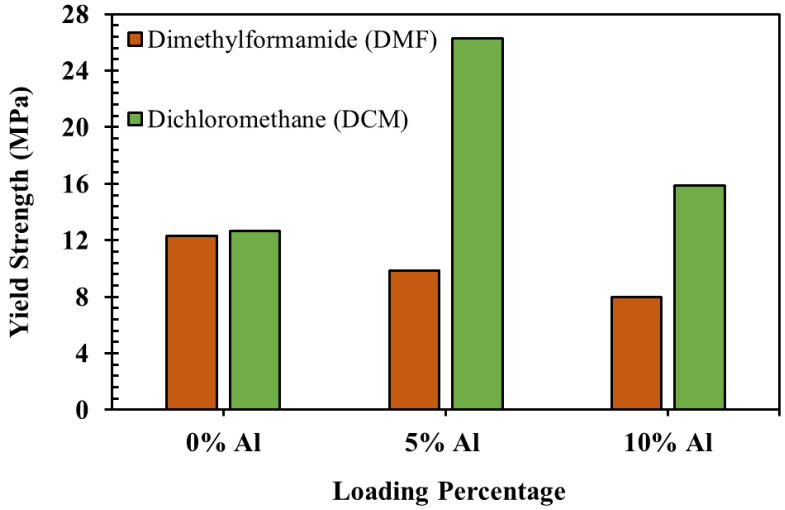

Figure 4. Comparison of yield strength (ASTM D638) of specimens prepared using DMF and DCM

3.2 Effect of 3D Printing

The field of 3D printing is still relatively new and hence there are no established standards for printing specimens to test mechanical properties. In order to determine the optimal print settings and orientation needed to obtain samples with maximum strength, the following process parameters were varied: layer height, number of shells, infill percentage, infill pattern, and orientation. The printer head speed and the extruder temperature were held constant. A summary of the experiments is provided in Table 2. The flat and on-edge orientation are shown in Fig. 5 (a) and (b) respectively.

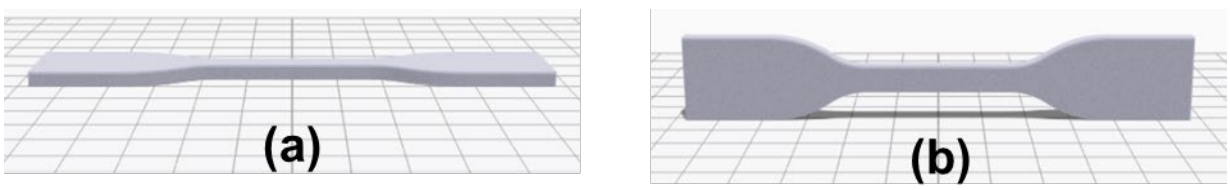

Figure 5. (a) Flat and (b) On-edge orientation for 3D printing

Table 2. Test settings for 3D printing dumbbell specimens

TEST NUMBER	LAYER HEIGHT	# OF SHELLS	INFILL %	INFILL PATTERN	ORIENTATION
1 (CONTROL)	0.21	3	95%	Diamond	Flat
2	0.21	3	95%	Linear	Flat
3	0.21	3	95%	Hexagonal	Flat
4	0.21	3	95%	Linear (Interleaved)	Flat
5	0.21	3	75%	Diamond	Flat
6	0.4	3	95%	Diamond	Flat
7	0.21	3	95%	Diamond	On-edge
8	0.21	2	95%	Diamond	Flat
9	0.4	3	95%	Diamond	On-edge

The maximum strength was obtained with the on-edge orientation which corresponds to Test 7 in Table 2. This orientation resulted in the 3D printer slicer print the specimen with the majority of the filaments oriented along the length of the specimen. This results in the applied force acting parallel to the filaments. Hence forth, this orientation was used for printing all specimens.

3.3 Effect of Nano Alumina Loading Percentage

The film samples obtained after solvent extraction were tested as per ASTM D882 and the results are shown in Figure 6. The results show that the yield strength of nanocomposite with 5 wt% alumina is highest with lesser strain whereas 10 wt% composite is harder and tougher with good strain hardening. The results also show that alumina affects elastic and plastic zones. This indicates that the addition of alumina affects the flexibility of polymer and increases the degree of crystallinity.

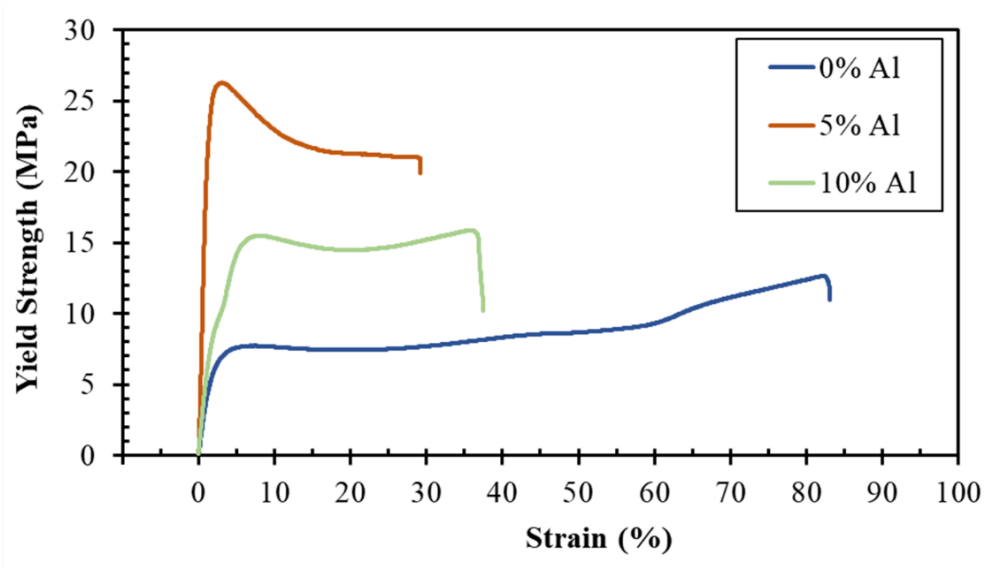

Figure 6. Stress-Strain curve of PLA – nano alumina film prepared using DCM and tested per ASTM D882

The results of ASTM D638 test on 3D printed dumbbell shaped specimens with varying weight compositions of alumina are shown in Figure 7. The results show that the addition of alumina did not improve the tensile strength of the 3D printed dumbbell specimens and it indicates that the alumina particles are affecting the flexibility of PLA after addition of heat in multiple stages. However, the slope of stress-strain curve showed that the 10 wt% and 5 wt% composites became tougher with moderate ductile behavior. Tensile strength at break (ultimate) values were same as tensile strength at yield and that confirmed that the samples had transformed into a brittle state and this degradation was caused due to the multiple heat – cool steps in the fabrication process. The first heat cycle is in the extruder and the second heat cycle is in the 3D printer.

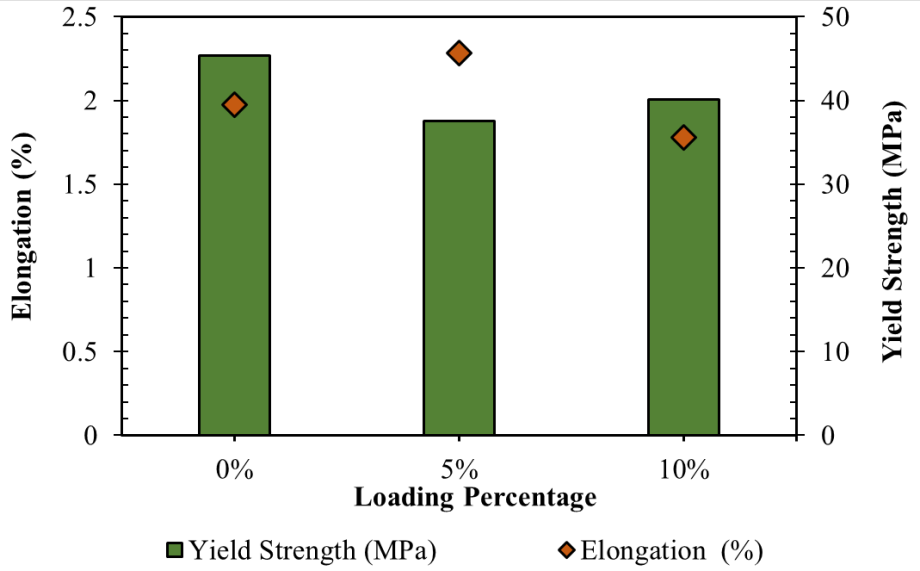

Figure 7. Comparison of yield strength and elongation for PLA-alumina nanocomposite dumbbell specimen prepared using DCM

3.4 Effect of Solid State Foaming

The average gas percentage in the film specimens after 2 hours of saturation was on an average 5%. The average pore size and porosity in the foamed samples (5 wt% alumina) were measured to be 50 μm and 80% respectively. The foamed film samples were tested as per ASTM D882 and the results are shown in Figure 8. The data show that the yield strength of 5 wt% and 10 wt% composite foams increased by 59% and 75% respectively from pure PLA foams. This shows that the nano alumina enhances the yield strength and elongation of foamed samples and there is good interaction between alumina and PLA. However, the elongation in 5 wt% composite foam is 18% higher than 10 wt% composite foams. This is caused due to the inconsistent porous structure in foamed filament across the cross section. It was also noted that 10 wt% alumina composite foams had larger pore sizes compared to other samples. This translates to the fact that the size and volume of porous structure contribute to the strength of foamed samples along with the nano alumina reinforcement.

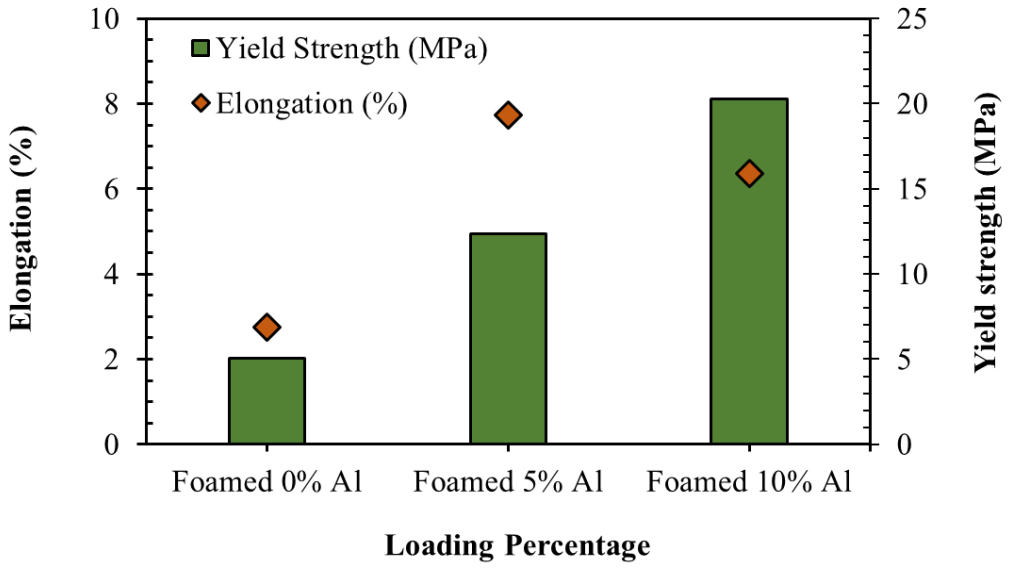

Figure 8. Comparison of yield strength and elongation for PLA - alumina nanocomposite foams prepared using DCM

4. CONCLUSIONS

In summary, a cost effective fabrication approach combining 3D printing and solid state foaming for obtaining nano alumina infused polymer foams with desired architectures was developed. The preliminary results indicate that DCM is the preferred solvent for fabricating PLA-alumina composites. The mechanical testing results showed that the 3D printed alumina infused polymer samples had lower strength than pure PLA, however, the polymer nanocomposite foams had better properties than pure PLA foams in both elongation at break and yield strength. The presence of alumina in the nano composites aids in bubble nucleation and also acts as a reinforcement improving the properties. This control over morphology of the foamed samples through additive manufacturing and solid state foaming translates to the ability to fabricate light weight composites with desired architectures for specific applications. Future work includes performing simulations using molecular dynamics to investigate the nonbinding interactions between PLA and alumina in the presence of dichloromethane.

5. REFERENCES

[1] Hoseini, A. H. A., Arjmand, M., Sundararaj, U., and Trifkovic, M. “Significance of Interfacial Interaction and Agglomerates on Electrical Properties of Polymer-Carbon Nanotube Nanocomposites.” *Materials & Design*, Vol. 125, 2017, pp. 126–134. https://doi.org/10.1016/j.matdes.2017.04.004.

[2] Fan, Q., Zhang, Q., Zhou, W., Xia, X., Yang, F., Zhang, N., Xiao, S., Li, K., Gu, X., Xiao, Z., Chen, H., Wang, Y., Liu, H., Zhou, W., and Xie, S. “Novel Approach to Enhance Efficiency of Hybrid Silicon-Based Solar Cells via Synergistic Effects of Polymer and Carbon Nanotube Composite Film.” *Nano Energy*, Vol. 33, 2017, pp. 436–444. https://doi.org/10.1016/j.nanoen.2017.02.003.

[3] Yanilmaz, M., Dirican, M., Asiri, A. M., and Zhang, X. “Flexible Polyaniline-Carbon Nanofiber Supercapacitor Electrodes.” *Journal of Energy Storage*, Vol. 24, 2019, p. 100766. https://doi.org/10.1016/j.est.2019.100766.

[4] Huang, X., Zhang, S., Xiao, W., Luo, J., Li, B., Wang, L., Xue, H., and Gao, J. “Flexible PDA@ACNTs Decorated Polymer Nanofiber Composite with Superhydrophilicity and Underwater Superoleophobicity for Efficient Separation of Oil-in-Water Emulsion.” *Journal of Membrane Science*, Vol. 614, 2020, p. 118500. https://doi.org/10.1016/j.memsci.2020.118500.

[5] Sengwa, R. J., Choudhary, S., and Dhatarwal, P. “Investigation of Alumina Nanofiller Impact on the Structural and Dielectric Properties of PEO/PMMA Blend Matrix-Based Polymer Nanocomposites.” *Advanced Composites and Hybrid Materials*, Vol. 2, No. 1, 2019, pp. 162–175. https://doi.org/10.1007/s42114-019-00078-8.

[6] Choudhary, S. “Structural, Morphological, Thermal, Dielectric, and Electrical Properties of Alumina Nanoparticles Filled PVA-PVP Blend Matrix-Based Polymer Nanocomposites.” *Polymer Composites*, Vol. 39, No. S3, 2018, pp. E1788–E1799. https://doi.org/10.1002/pc.24793.

[7] Jiang, W., Sundarram, S. S., Wong, D., Koo, J. H., and Li, W. “Polyetherimide Nanocomposite Foams as an Ablative for Thermal Protection Applications.” *Composites Part B: Engineering*, Vol. 58, 2014, pp. 559–565. https://doi.org/10.1016/j.compositesb.2013.10.040.

[8] Guo, F., Aryana, S., Han, Y., and Jiao, Y. “A Review of the Synthesis and Applications of Polymer–Nanoclay Composites.” *Applied Sciences*, Vol. 8, No. 9, 2018, p. 1696. https://doi.org/10.3390/app8091696.

[9] Wang, H., Yang, X., Fu, Z., Zhao, X., Li, Y., and Li, J. “Rheology of Nanosilica-Compatibilized Immiscible Polymer Blends: Formation of a ‘Heterogeneous Network’ Facilitated by Interfacially Anchored Hybrid Nanosilica.” *Macromolecules*, Vol. 50, No. 23, 2017, pp. 9494–9506. https://doi.org/10.1021/acs.macromol.7b02143.

[10] Wei, Q., Wang, Y., Rao, Y., Jiang, A., Zhang, K., Lu, T., and Chen, X. “Evaluating the Effects of Nanosilica on Mechanical and Tribological Properties of Polyvinyl Alcohol/Polyacrylamide Polymer Composites for Artificial Cartilage from an Atomic Level.” *Polymers*, Vol. 11, No. 1, 2019, p. 76. https://doi.org/10.3390/polym11010076.

[11] Hamidinejad, M., Zhao, B., Zandieh, A., Moghimian, N., Filleter, T., and Park, C. B. “Enhanced Electrical and Electromagnetic Interference Shielding Properties of Polymer–Graphene Nanoplatelet Composites Fabricated via Supercritical-Fluid Treatment and Physical Foaming.” *ACS Applied Materials & Interfaces*, Vol. 10, No. 36, 2018, pp. 30752–30761. https://doi.org/10.1021/acsami.8b10745.

[12] Payandehpeyman, J., Mazaheri, M., and Khamehchi, M. “Prediction of Electrical Conductivity of Polymer-Graphene Nanocomposites by Developing an Analytical Model Considering Interphase, Tunneling and Geometry Effects.” *Composites Communications*, Vol. 21, 2020, p. 100364. https://doi.org/10.1016/j.coco.2020.100364.

[13] Wang, Q., Wang, Y., Meng, Q., Wang, T., Guo, W., Wu, G., and You, L. “Preparation of High Antistatic HDPE/Polyaniline Encapsulated Graphene Nanoplatelet Composites by Solution Blending.” *RSC Advances*, Vol. 7, No. 5, 2017, pp. 2796–2803. https://doi.org/10.1039/C6RA26458A.

[14] Oyarzabal, A., Cristiano-Tassi, A., Laredo, E., Newman, D., Bello, A., Etxeberría, A., Eguiazabal, J. I., Zubitur, M., Mugica, A., and Müller, A. J. “Dielectric, Mechanical and

Transport Properties of Bisphenol A Polycarbonate/Graphene Nanocomposites Prepared by Melt Blending." *Journal of Applied Polymer Science*, Vol. 134, No. 13, 2017. https://doi.org/10.1002/app.44654.

[15] Shen, H., Wang, S., Xu, H., Zhou, Y., and Gao, C. "Preparation of Polyamide Thin Film Nanocomposite Membranes Containing Silica Nanoparticles via an In-Situ Polymerization of SiCl4 in Organic Solution." *Journal of Membrane Science*, Vol. 565, 2018, pp. 145–156. https://doi.org/10.1016/j.memsci.2018.08.016.

[16] Eaves, D. *Polymer Foams-Trends in Use and Technology*. Smithers Rapra Press, Shawbury, UK, 1996.

[17] Miller, D., Chatchaisucha, P., and Kumar, V. "Microcellular and Nanocellular Solid-State Polyetherimide (PEI) Foams Using Sub-Critical Carbon Dioxide I. Processing and Structure." *Polymer*, Vol. 50, No. 23, 2009, pp. 5576–5584. https://doi.org/10.1016/j.polymer.2009.09.020.

[18] Lee, L., Zeng, C., Cao, X., Han, X., Shen, J., and Xu, G. "Polymer Nanocomposite Foams." *Composites Science and Technology*, Vol. 65, Nos. 15–16, 2005, pp. 2344–2363. https://doi.org/10.1016/j.compscitech.2005.06.016.

[19] Janik, H., and Marzec, M. "A Review: Fabrication of Porous Polyurethane Scaffolds." *Materials Science and Engineering: C*, Vol. 48, 2015, pp. 586–591. https://doi.org/10.1016/j.msec.2014.12.037.

[20] Suh, S. W., Shin, J. Y., Kim, J., Kim, J., Beak, C. H., Kim, D.-I., Kim, H., Jeon, S. S., and Choo, I.-W. "Effect of Different Particles on Cell Proliferation in Polymer Scaffolds Using a Solvent-Casting and Particulate Leaching Technique:" *ASAIO Journal*, Vol. 48, No. 5, 2002, pp. 460–464. https://doi.org/10.1097/00002480-200209000-00003.

[21] Day, R. M., Boccaccini, A. R., Maquet, V., Shurey, S., Forbes, A., Gabe, S. M., and Jérôme, R. "In Vivo Characterisation of a Novel Bioresorbable Poly(Lactide-Co-Glycolide) Tubular Foam Scaffold for Tissue Engineering Applications." *Journal of Materials Science: Materials in Medicine*, Vol. 15, No. 6, 2004, pp. 729–734. https://doi.org/10.1023/B:JMSM.0000030216.73274.86.

[22] Kim, Y.-H., and Li, W. "Multifunctional Polyetherimide Nanocomposite Foam." *Journal of Cellular Plastics*, Vol. 49, No. 2, 2013, pp. 131–145. https://doi.org/10.1177/0021955X13477434.

[23] Kakumanu, V., and Srinivas Sundarram, S. "Dual Pore Network Polymer Foams for Biomedical Applications via Combined Solid State Foaming and Additive Manufacturing." *Materials Letters*, Vol. 213, 2018, pp. 366–369. https://doi.org/10.1016/j.matlet.2017.11.027.

[24] Guo, H., and Kumar, V. "Solid-State Poly(Methyl Methacrylate) (PMMA) Nanofoams. Part I: Low-Temperature CO2 Sorption, Diffusion, and the Depression in PMMA Glass Transition." *Polymer*, Vol. 57, 2015, pp. 157–163. https://doi.org/10.1016/j.polymer.2014.12.029.

[25] Aher, B., Olson, N. M., and Kumar, V. "Production of Bulk Solid-State PEI Nanofoams Using Supercritical CO2." *Journal of Materials Research*, Vol. 28, No. 17, 2013, pp. 2366–2373. https://doi.org/10.1557/jmr.2013.108.

[26] Wang, G., Wan, G., Chai, J., Li, B., Zhao, G., Mu, Y., and Park, C. B. "Structure-Tunable Thermoplastic Polyurethane Foams Fabricated by Supercritical Carbon Dioxide Foaming and Their Compressive Mechanical Properties." *The Journal of Supercritical Fluids*, Vol. 149, 2019, pp. 127–137. https://doi.org/10.1016/j.supflu.2019.04.004.

[27] Rahim, T. N. A. T., Abdullah, A. M., and Md Akil, H. “Recent Developments in Fused Deposition Modeling-Based 3D Printing of Polymers and Their Composites.” *Polymer Reviews*, Vol. 59, No. 4, 2019, pp. 589–624. https://doi.org/10.1080/15583724.2019.1597883.
[28] Serra, T., Mateos-Timoneda, M. A., Planell, J. A., and Navarro, M. “3D Printed PLA-Based Scaffolds: A Versatile Tool in Regenerative Medicine.” *Organogenesis*, Vol. 9, No. 4, 2013, pp. 239–244.
[29] Department of Mechanical Design Eng., KIT UNIV., Kang, Y.-G., Lee, T.-W., and Shin, G.-S. “The Influence of Experiment Variables on 3D Printing Using ABS Resin.” *The Korean Society of Manufacturing Process Engineers*, Vol. 16, No. 2, 2017, pp. 94–101. https://doi.org/10.14775/ksmpe.2017.16.2.094.
[30] NatureWorks LLC Home Page. http://www.natureworksllc.com/. Accessed Feb. 15, 2012.
[31] Jose, D., Gutierrez, C., and Srinivas Sundarram, S. Fabrication of Bulk Skinless Polyetherimide (PEI) Nanofoams. Phoenix, AZ, 2016.
[32] *ASTM D882-18, Standard Test Method for Tensile Properties of Thin Plastic Sheeting*. ASTM International, West Conshohocken, PA, 2018.
[33] *ASTM D638-14, Standard Test Method for Tensile Properties of Plastics*. ASTM International, West Conshohocken, PA, 2014.

Appendix – A

Table 3. Summary of all experiments

Case	Solvent	PLA weight (g)	PLA: Solvent ratio	Alumina wt %	Ultrasonic Stirring		Extrusion			Solid State Foaming	
					Power (W)	Duration (min)	Temperature T1 (°C)	Temperature T2 (°C)	Motor Speed (rpm)	Pressure (MPa)	Temp (°C)
1	DCM	10	1:12	0	125	60	170	170	15	2.5	90
2	DCM	10	1:12	5	125	60	170	170	15	2.5	90
3	DCM	10	1:12	10	125	60	170	170	15	2.5	90
4	DMF	10	1:12	0	125	60	170	170	15	2.5	90
5	DMF	10	1:12	5	125	60	170	170	15	2.5	90
6	DMF	10	1:12	10	125	60	170	170	15	2.5	90

A minimum of 3 samples were processed for each case.